

Solution of Analytical-Variational Method on Bi-Material Interface Crack and Its Comparison with Experiment

Qingchun Meng*, Dong-Joo Lee** and Xing Zhang*

(Received November 25, 1996)

An analytical method is developed to describe the fields of stress and displacement in a bi-material strip with an edge interfacial crack. All of the basic governing equations, boundary conditions on crack surfaces, and conditions of continuity along the interface are satisfied by the eigen-function expansion method. The other boundary conditions will be satisfied by the generalized variational principle. Good convergence of generalized stress intensity factors is obtained, and the values of crack opening displacement and energy release rate obtained by this method are close to the experimental results. Some problems regarding oscillatory singularity, contact zone and energy release rate are discussed. Finally, the effects of modulus, thickness and crack length to mode mixity are presented.

Key Words: Interface Crack, Analytical Variational Method, Stress Intensity Factor, Energy Release Rate, Crack Opening Displacement, Bi-Material Strip

1. Introduction

The stress field in the vicinity of an interfacial crack tip between dissimilar media was analyzed by Williams (1959), who also determined the characteristic oscillating stress singularity. This phenomenon was confirmed by solutions to specific problems as given by Erdogan (1965), England (1965), Rice and Sih (1965). The penetration between the upper and lower surfaces of a crack was found by England (1965). In 1988, Rice published his review on interfacial cracks, in which problems related to near-tip stress field, definition of stress intensity factors, contact zone, etc. are discussed. It must be mentioned that the interface crack problems are mixed-mode ones in most cases, so the stress fields are governed by multi-mechanical parameters. Therefore, the numerical simulations are only useful when the corresponding single parameter fracture criterion

is valid.

Since then, there have been a lots of papers published on interfacial cracks, e.g., Choi (1994). To find a simple and effective technique for an interface crack problem encountered in engineering, Meng and Zhang (1992) have developed the analytical-variational method of solution to determine the generalized stress intensity factors (GSIFs) of the interface crack in bi-metal glued joints. In their analysis, the eigen expansions of displacement and stress field satisfying all the basic governing equations in mechanics of elasticity, boundary conditions on crack surfaces and conditions of continuity along the interface are first derived by the eigen-function expansion method. Furthermore, the other boundary conditions excluding those in which the crack surfaces are satisfied by the generalized variational principle, then a simultaneous equations with all the coefficients in the expansions of displacement and stress is obtained. Finally, all coefficients are determined and the coefficients of the leading two terms are designated as the generalized stress intensity factors, which converge after enough terms have been taken in the expansion.

This *analytical variational method* can be used

* Box 508, Beijing University of Aeronautics and Astronautics, Beijing, 100083, P. R. China

** Yeungnam University, Dept. of Mechanical Engineering, Daedong, Gyungsan, 712-749, Korea

to analyse the strength of structures with interface cracks, such as single and double strip glued joints in aircraft structures, and to understand the requirement of damage tolerance design. Furthermore, the same approach can be used to deal with delamination problems, which is the main form of failure in composite laminated plates.

Compared to other methods, this method ensures that all the governing equations and boundary conditions on the crack surfaces and conditions of continuity along the interface are satisfied exactly. There are only line integrals in the variational equations, so that the computations are very simple.

Choi and Chai (1995) presented their experimental results on bimaterial interface crack, in which the specimen geometry used was an edge-cracked bimaterial strip, which gave rise to crack length independence of fracture parameters and mode-mixities. They developed a hybrid procedure for extracting stress intensity factors, and found a large increase in toughness as the shear components of displacement increased.

In this paper, the crack opening displacements and energy release rate of the interface crack in bimaterial are calculated using the analytical-variational method, and compared with the experimental results measured by Choi and Chai (1995).

2. Eigen Expansions of Stress and Displacement Fields

According to the theory of Muskhelishvili (1953), for an isotropic plane problem the general solution of stress and displacement in both material satisfying all of the basic equations in elasticity mechanics are given by

$$2\mu(u_x + iu_y) = \chi\phi(z) - (z - \bar{z})\overline{\phi'(z)} - \overline{\Omega(z)} \quad (1)$$

$$\sigma_{yy} - i\sigma_{xy} = \phi'(z) + (z - \bar{z})\overline{\phi''(z)} + \overline{\Omega'(z)} \quad (2)$$

$$\sigma_{xx} + \sigma_{yy} = 2\{\phi'(z) + \overline{\phi'(z)}\} \quad (3)$$

where, μ is the shear modulus, χ is given by $(3-4\nu)$ in plane strain and $(3-\nu)/(1+\nu)$ in plane stress, and ν is Poisson's ratio. The func-

tions $\phi(z)$ and $\Omega(z)$, where $z = x + iy$, are analytic, $\phi'(z) = d\phi/dz$, and the overbar denotes complex conjugation. According to Meng and Zhang (1992), these functions are taken as a combination of power and exponential functions:

$$\left. \begin{aligned} \phi_k(z) &= A_k z^\lambda + B_k z^{\lambda} + E_k e^{\lambda z} + F_k e^{\bar{\lambda} z} \\ \Omega_k(z) &= C_k z^\lambda + D_k z^{\bar{\lambda}} + G_k e^{\lambda z} + H_k e^{\bar{\lambda} z} \end{aligned} \right\} \quad (4)$$

where the subscripts $k=1$ and 2 refer to the upper and lower material in a bi-material strip; λ is a complex eigenvalue and all of the coefficients are complex quantities.

The conditions of continuity along the interface and the boundary conditions on the crack surfaces are given as

$$\left. \begin{aligned} (u_x + iu_y)_1 &= (u_x + iu_y)_2 & \theta &= 0 \\ (\sigma_{yy} - i\sigma_{xy})_1 &= (\sigma_{yy} - i\sigma_{xy})_2 & \theta &= 0 \\ (\sigma_{yy} - i\sigma_{xy})_1 &= 0 & \theta &= \pi \\ (\sigma_{yy} - i\sigma_{xy})_2 &= 0 & \theta &= -\pi \end{aligned} \right\} \quad (5)$$

where the subscripts 1 and 2 denote different materials, respectively. All the conditions should be satisfied by both of the two groups of stress and displacement which are determined by the power and exponential functions mentioned above. Then, two groups of simultaneous equations with the complex coefficients introduced in Eq. (4) can be established.

Based on the conditions for a non-trivial solution to these equations, the eigenvalues can be determined. For power functions, there are two groups of eigenvalues. The first one is complex (e. g. see Rice, 1988),

$$\lambda = \frac{n}{2} + i\varepsilon \quad n=1, 3, 5, \dots \quad (6)$$

$$\varepsilon = \frac{1}{2n} \ln \frac{\mu_1 + \mu_2 \chi_1}{\mu_2 + \mu_1 \chi_2} \quad (7)$$

in which ε is the *bimaterial constant*. The second group is real,

$$\lambda = \frac{n}{2} \quad n=2, 4, 6, \dots \quad (8)$$

For exponential functions, it can be found that the non-trivial solution exists as long as $\lambda \neq 0$. For simplicity, it is taken as $\lambda=1$.

After an involved derivation, the eigen expansions of the whole field of stress and displacement

are obtained as follows:

$$\begin{aligned}
 u_{ik} &= \sum_{m=1}^M r^{m-\frac{1}{2}} \{ [P_m^R S_{ikm}^R(\theta) \\
 &+ P_m^I S_{ikm}^I(\theta)] \cos(\varepsilon \ln r) \\
 &+ [-P_m^R S_{ikm}^I(\theta) + P_m^I S_{ikm}^R(\theta)] \sin(\varepsilon \ln r) \} \\
 &+ \sum_{m=1}^M r^m \{ Q_m^R t_{ikm}^R(\theta) + Q_m^I t_{ikm}^I(\theta) \} \\
 &+ R^R q_{ik}^R(r, \theta) + R^I q_{ik}^I(r, \theta) \quad (9) \\
 \sigma_{ijk} &= \sum_{m=1}^M r^{m-\frac{3}{2}} \{ [P_m^R g_{ijkm}^R(\theta) \\
 &+ P_m^I g_{ijkm}^I(\theta)] \cos(\varepsilon \ln r) \\
 &+ [-P_m^R g_{ijkm}^I(\theta) + P_m^I g_{ijkm}^R(\theta)] \sin(\varepsilon \ln r) \} \\
 &+ \sum_{m=1}^M r^{m-1} \{ Q_m^R h_{ijkm}^R(\theta) \\
 &+ Q_m^I h_{ijkm}^I(\theta) \} + R^R p_{ijk}^R(r, \theta) \\
 &+ R^I p_{ijk}^I(r, \theta) \quad (10)
 \end{aligned}$$

in which all of the functions with θ or r and θ are known functions. The unknown coefficients in front of these functions will be determined using the generalized variational principle, to satisfy the other boundary conditions excluding those on the crack surfaces.

3. Near-Tip Analysis

3.1 Near-tip stress field

The singular stress fields in the vicinity of a crack tip are governed by the coefficients of the leading terms P_1^R and P_1^I , so the two parameters P_1^R and P_1^I can be called *generalized stress intensity factors* (GSIFs). The components of stress along $\theta=0$ are given by

$$\begin{aligned}
 \sigma_{yy} \Big|_{\theta=0} &= \frac{1+\eta}{2} \eta r^{-\frac{1}{2}} \{ (P_1^R + 2\varepsilon P_1^I) \cos(\varepsilon \ln r) \\
 &- (2\varepsilon P_1^R - P_1^I) \sin(\varepsilon \ln r) \} \\
 \sigma_{xy} \Big|_{\theta=0} &= \frac{1+\eta}{2} \eta r^{-\frac{1}{2}} \{ (2\varepsilon P_1^R - P_1^I) \cos(\varepsilon \ln r) \\
 &+ (P_1^R + 2\varepsilon P_1^I) \sin(\varepsilon \ln r) \}
 \end{aligned}$$

in which $\eta = (\mu_1 + \mu_2 \chi_1) / (\mu_2 + \mu_1 \chi_2)$, and the subscript k has been ignored because of the continuity of stresses along $\theta=0$.

Let

$$\left. \begin{aligned}
 k_1 &= \frac{\sqrt{2\pi}}{2} (1+\eta) (P_1^R + 2\varepsilon P_1^I) \\
 k_2 &= \frac{\sqrt{2\pi}}{2} (1+\eta) (2\varepsilon P_1^R - P_1^I)
 \end{aligned} \right\} \quad (11)$$

The complex SIF can be defined as $K = k_1 + ik_2$ (Rice, 1988). Then

$$(\sigma_{yy} + i\sigma_{xy}) \Big|_{\theta=0} = \frac{K}{\sqrt{2\pi r}} r^{i\varepsilon} \quad (12)$$

where k_1 and k_2 are another group of GSIF. The mode mixity Ψ is defined as

$$\Psi = \tan^{-1} \frac{\text{Im}[K r^{i\varepsilon}]}{\text{Re}[K r^{i\varepsilon}]} \quad (13)$$

According to the suggestion of Rice (Rice, 1988), the distance from the crack-tip r in Eq. (13) should be taken as 1.0 micrometer in the calculation of mode-mixity Ψ .

Along the crack surfaces,

$$\begin{aligned}
 (u_{y1} + iu_{x1})_{\theta=\pi} - (u_{y2} + iu_{x2})_{\theta=-\pi} \\
 = \frac{(1+\eta)(c_1+c_2)}{4\sqrt{r} \cosh(\pi\varepsilon)} (P_1^R - iP_1^I) r^{i\varepsilon} \\
 = \frac{(c_1+c_2)(k_1+ik_2)r^{i\varepsilon}}{2\sqrt{2\pi r}(1+2i\varepsilon)\cosh(\pi\varepsilon)}
 \end{aligned}$$

In which $c_1 = (\chi_1 + 1) / \mu_1$ and $c_2 = (\chi_2 + 1) / \mu_2$. The energy release rate was given by Malyshev and Salganik (1965) and Rice (1988), and is derived in this paper as:

$$\begin{aligned}
 G &= \frac{(1+\eta)^2 (c_1+c_2) \pi}{32 \cosh^2(\pi\varepsilon)} [(P_1^R)^2 + (P_1^I)^2] \\
 &= \frac{(c_1+c_2)}{16 \cosh^2(\pi\varepsilon)} (k_1^2 + k_2^2) \quad (14)
 \end{aligned}$$

3.2 Small contact zone

Generally the bimaterial constant $\varepsilon \neq 0$, and the stress fields have oscillatory behavior in the vicinity of a crack tip. Due to the existence of an oscillatory singularity, there is penetration between the surfaces of the crack as indicated by England (1965). Because of the satisfaction of both the free boundary conditions on crack surfaces and the conditions of continuity along the interface, such a phenomenon cannot be avoided in most cases. Certainly, this behavior is unreasonable, but the zone in which the interpenetration occurs is so small that the effect of interpenetration can be ignored except in the case of pure shearing mode (Rice, 1988).

The size of the contact zone near the tip can be estimated using the expansions of displacement. From Eq. (9), the crack opening displacement in the vicinity of the crack tip is written as:

$$\begin{aligned} \Delta u_y &= u_{y1} \Big|_{\theta=\pi} - u_{y2} \Big|_{\theta=-\pi} \\ &= c r^{\frac{1}{2}} \sqrt{(P_1^R)^2 + (P_1^I)^2} \sin(\varepsilon \ln r + \gamma) \end{aligned} \quad (15)$$

where

$$\begin{aligned} c &= \left(\frac{\chi_1}{\mu_1} + \frac{1}{\mu_2} \right) (e^{\pi\varepsilon} + e^{-\pi\varepsilon}), \\ \text{and } \tan \gamma &= \frac{P_1^R}{P_1^I} \end{aligned} \quad (16)$$

The size of contact zone is estimated by

$$r_c = \exp\left(\frac{n\pi - \gamma}{\varepsilon}\right), \quad n=0, \pm 1, \dots \quad (17)$$

The magnitude of r_c will be presented later.

If both bimetaterials are incompressible (i. e. $\nu_1 = \nu_2 = 0.5$), it will be found that $\varepsilon = 0$. In this case, the oscillatory singularity reduces to the monotonic type and there is no penetration. The SIF can be defined as

$$K_{I1} = k_1 = \sqrt{2\pi} P_1^R \quad K_{II1} = k_2 = \sqrt{2\pi} P_1^I \quad (18)$$

and the near tip stress fields are

$$\sigma_{yy} \Big|_{\theta=0} = \frac{K_{I1}}{\sqrt{2\pi r}} \quad \sigma_{xy} \Big|_{\theta=0} = -\frac{K_{II1}}{\sqrt{2\pi r}} \quad (19)$$

It can be seen that the expression of both stress intensity factors and near-tip stress fields are the same as the classical type.

4. Variational Method of Solution

The coefficients P_m^R , P_m^I , Q_m^R , Q_m^I , R^R and Eqs. (9) and (10) are determined from the boundary conditions excluding those on the crack surfaces. According to the generalized variational principle for multi-regions (Qian, 1980),

$$\begin{aligned} \delta \Pi_g &= \sum_{k=1}^2 \int_{V_k} \left[\frac{\partial W}{\partial \varepsilon_{ij}} - \sigma_{ij} \right]_k \delta \varepsilon_{ijk} dv \\ &\quad - \sum_{k=1}^2 \int_{V_k} \left[\varepsilon_{ij} - \frac{1}{2} \left(\frac{\partial u_i}{\partial x_j} + \frac{\partial u_j}{\partial x_i} \right) \right]_k \delta \sigma_{ijk} dv \\ &\quad - \sum_{k=1}^n \int_{V_k} \left[\frac{\partial \sigma_{ij}}{\partial x_j} + B_i \right]_k \delta u_{ik} dv \\ &\quad + \sum_{k=1}^2 \int_{S_{pk}} (\sigma_{ij} n_j - \bar{p}_i)_k \delta u_{ik} ds \\ &\quad - \sum_{k=1}^2 \int_{S_{uk}} (u_i - \bar{u}_i)_k \delta \sigma_{ijk} n_{jk} ds \\ &\quad + \int_{S^*} (\sigma_{i1} n_{j1} + \sigma_{i2} n_{j2}) \delta u_{i1} ds \\ &\quad + \int_{S^*} (u_{i1} - u_{i2}) \delta \sigma_{i2} n_{j2} ds = 0 \end{aligned} \quad (20)$$

in which, $\delta \Pi_g$ is the variation of functional Π_g ;

S^* denotes the interface; S_{pk} and S_{uk} refer to the boundary with prescribed surface traction and displacements in material k , respectively; \bar{p}_{ik} and \bar{u}_{ik} denote the known traction and displacement.

In this problem, all the basic governing equations, boundary conditions on crack surfaces, and conditions of continuity along the interface are exactly satisfied a priori, so Eq. (20) is simplified as follows (Meng and Zhang, 1992)

$$\begin{aligned} &\sum_{k=1}^n \int_{S_{pk}} (\sigma_{ij} n_j - \bar{p}_i)_k \delta u_{ik} ds \\ &- \sum_{k=1}^2 \int_{S_{uk}} (u_i - \bar{u}_i)_k \delta \sigma_{ijk} n_{jk} ds = 0 \end{aligned} \quad (21)$$

This is equivalent to the boundary conditions excluding those on the crack surfaces.

Substituting Eqs. (9) and (10) into Eq. (21), the linear algebraic simultaneous equations with all of the coefficients can be established as follows:

$$\begin{aligned} \sum_{m=1}^M \sum_{n=1}^4 \lambda_{pqmn} \zeta_{mn} + \sum_{l=1}^2 \lambda_{pql} \zeta_l &= \Delta_{pq} \quad \left\{ \begin{array}{l} p=1, 2, \dots, M \\ q=1, 2, 3, 4 \end{array} \right. \\ \sum_{m=1}^M \sum_{n=1}^4 \mu_{rnm} \zeta_{mn} + \sum_{l=1}^2 \mu_{rl} \zeta_l &= \Delta_r, \quad r=1, 2 \end{aligned} \quad (22)$$

Here

$$\begin{aligned} \zeta_1 &= R^R, \quad \zeta_2 = R^I, \quad \zeta_{m1} = P_m^R, \quad \zeta_{m2} = P_m^I, \quad \zeta_{m3} \\ &= Q_m^R, \quad \zeta_{m4} = Q_m^I \end{aligned}$$

and M is the number of terms taken in the expansion of displacements and stresses. The other quantities are integrals along the boundary except crack surfaces which are obtained from Eq. (21) by means of numerical integration.

Solving Eq. (22), all of the coefficients in the expansions of stress and displacement field will be determined, including the GSIFs P_1^R and P_1^I .

5. Numerical Results and Comparison with Experiment

Recently, Choi and Chai (1995) used the bi-material strip specimen which is glued by epoxy and glass with an edge crack laying along the interface. The normal crack opening displacements (NCOD) under different biaxial loading were measured by crack opening interferometer. The mechanics model of such a specimen in this experiment is shown in Fig. 1. The specimen was

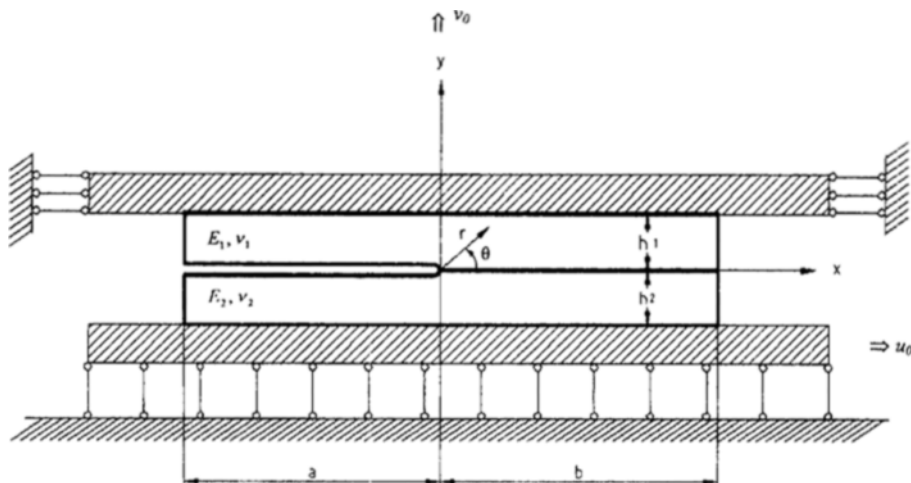


Fig. 1 The mechanics model of bimaterial strip under biaxial loading

glued along the edges to two sets of grip plates (expressed as the shaded region in Fig. 1) which provide uniform displacements u_0 and v_0 to lower and upper edges along the x - and y -axis, respectively. The upper material is epoxy with $E_1=1.72$ GPa and $\nu_1=0.4$, and the lower material is glass with $E_2=68.95$ GPa and $\nu_2=0.2$. In this case the bimaterial constant $\epsilon=0.0486476$. They performed a series of experiments applying normal loading and sequential shear loading, and obtained a sequence of NOCODs profiles from the center of various interference patterns corresponding to the center of a specimen far away from any edge effects. However, they presented three cases of NCOD profiles that presumably good results in their paper.

For the theoretical predication, a special program is written to perform the numerical analysis. To compare these predictions with the experimental data, the size of the specimen is selected as follows : the length of crack and ligament $a=b=$

75.0 mm, and the thickness of strip $h_1=h_2=10.0$ mm, so that it is the same as the values used in the experiments. To reduce the error in computation, the unit of size is taken as decimeters. Thus, the sizes of model become $a=b=0.75$ dm and $h_1=h_2=0.1$ dm. To be consistent with the experiment, the unit of length in Eqs. (13) and (14) should be converted to micrometer when the mode mixity Ψ and energy release rate G are calculated. The convergence of GSIFs (P_I^R and P_I^I) with M , the number of terms selected in the expansions, and the comparisons of CODs and G as the results of calculation and experiment, will be shown in the following tables and diagrams for different loading cases.

5.1 Comparisons with experiment

If the theoretical analysis is performed identical to the experimental steps, the following results are obtained :

Case 1. $u_0=0, v_0=6.65 \mu\text{m}$;

Table 1 The convergence of GSIFs in case of $u_0=0, v_0=6.65 \mu\text{m}$

M	5	6	7	8	9	10	11	12	13	14	15
$P_I^R \times 10^4$	0.576	2.147	2.138	2.046	1.794	1.984	1.946	2.149	1.974	1.935	1.986
$P_I^I \times 10^4$	-0.505	-0.355	-0.480	-0.550	-0.531	-0.488	-0.561	-0.855	-0.525	-0.603	-0.542

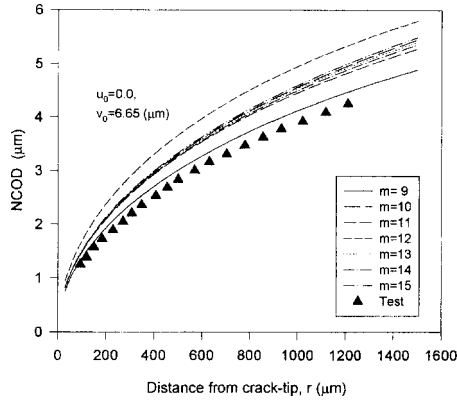


Fig. 2 The convergence of NCOD for different M , and its comparison with experiment

The CODs in this case are shown in Fig. 2. As shown, the results are quite similar to each other.

Taking $M=13$ and $P_1^R=1.974 \times 10^{-4}$, $P_1^I=-0.525 \times 10^{-4}$, from Eq. (17) the maximum possible (i. e., the size limited by crack length) size of the contact zone is found to be $r_c=4.5 \times 10^{-17}(\text{dm})$ and $r_c/a=6.0 \times 10^{-17}$. These results

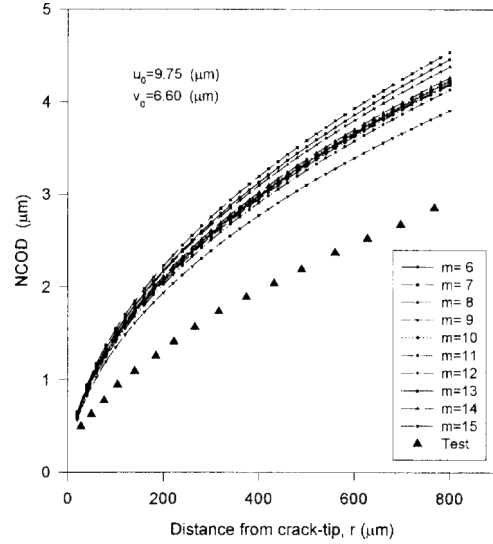


Fig. 3 The convergence of NCOD for different M , and its comparison with experiment

show that the contact zone is very small and its effect on the solution can be ignored.

Case 2. $u_0=9.75 \mu\text{m}$, $v_0=6.60 \mu\text{m}$;

Table 2 The convergence of GSIFs in case of $u_0=9.75 \mu\text{m}$, $v_0=6.65 \mu\text{m}$

M	5	6	7	8	9	10	11	12	13	14	15
$P_1^R \times 10^4$	0.324	2.439	2.454	2.380	2.147	2.305	2.281	2.256	2.297	2.291	2.288
$P_1^I \times 10^4$	0.627	0.783	0.669	0.629	0.588	0.588	0.650	0.676	0.607	0.491	0.603

The CODs in this case are shown in Fig. 3. As shown, the results are not as close as the previous case. However, the remote contact during pre-loading or measuring point selection in front of crack for experimental works can be a source for this discrepancy. Also, this approach that uses the elastic behavior of material can be another source

of this loading case. While applying positive shear loading, prior to normal loading there seems to be some non-linear effects in the vicinity of the crack-tip.

Taking $M=11$, $P_1^R=2.281 \times 10^{-4}$, $P_1^I=0.65 \times 10^{-4}$, we have $r_c=2.852 \times 10^{-12}(\text{dm})$ and $r_c/a=3.8 \times 10^{-12}$.

Case 3. $u_0=-9.47 \mu\text{m}$, $v_0=5.50 \mu\text{m}$;

Table 3 The convergence of GSIFs in case of $u_0=-9.47 \mu\text{m}$, $v_0=5.5 \mu\text{m}$

M	5	6	7	8	9	10	11	12	13	14	15
$P_1^R \times 10^4$	0.718	1.477	1.446	1.354	1.126	1.315	1.266	1.642	1.305	1.255	1.333
$P_1^I \times 10^4$	-1.514	-1.397	-1.510	-1.596	-1.522	-1.446	-1.636	-2.159	-1.529	-1.514	-1.554

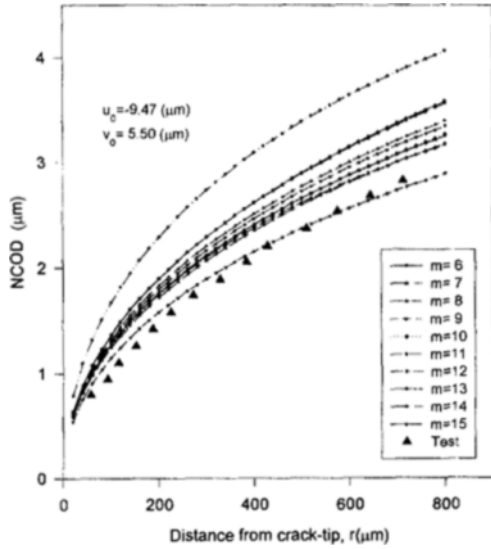


Fig. 4 The convergence of NCOD for different M , and its comparison with experiment

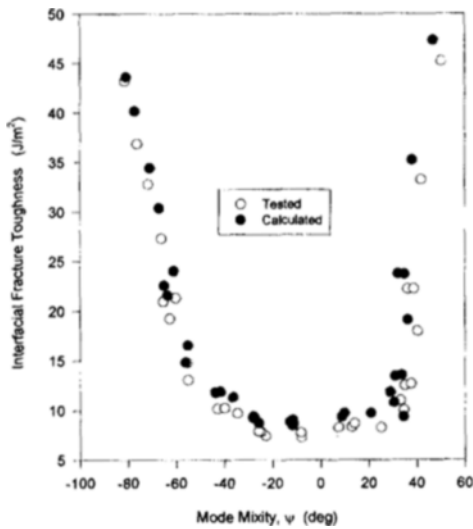


Fig. 5 The calculated energy release rate and tested interfacial fracture toughness, with respect to mode mixity

As in the first loading case, the theoretical results show quite similar results to those of the experiment in Fig. 4. Taking $M=15$, $P_1^R=1.333 \times 10^{-4}$, $P_1^I=-1.554 \times 10^{-4}$, the size of the contact zone is obtained as $r_c=1.92 \times 10^{-22}(\text{dm})$, $r_c/a=2.56 \times 10^{-22}$.

In the experiment (Choi and Chai, 1995),

different normal and shear displacements were applied until the interface crack extension occurred, upon which they obtained the interfacial fracture toughness. In this paper, the same normal and shear displacements are used to determine the GSIFs; furthermore, the relative energy release rates are obtained by Eq. (14). Figure 5 shows the relationship between the interfacial fracture toughness (energy release rate) and mode mixity obtained in the experimental test (Choi and Chai, 1995) and the theoretical computation in this paper, respectively.

The above results show, however, that : 1) the convergence of GSIFs with the increasing of M is satisfactory ; 2) the maximum possible size of the contact zone r_c is so small that the effect of the contact zone on the solution can be ignored ; 3) the normal CODs are convergent in every case ; 4) the CODs obtained in this paper are close enough to the experimental data presented by Choi and Chai (1995) only when a normal displacement v_0 is applied. But, after positive shear displacements are applied, the maximum error between experimental results and theoretical computation is nearly 30 %. Since the length of the crack is much longer than the thickness and the normal displacements are very small, the possibility exists that the crack surfaces contact each other nearby the remote edge of the crack when shear displacements are applied in the experiments. Such a contact may be a cause of this difference in the measurement of CODs. Also, there are several other possibilities such as crack growing pattern, selection of measuring point, differences in testing temperature and non-uniformity in specimens ; 5) the energy release rates calculated herein match the experimental results very well.

5.2 Further computational results

The relationship between the mode mixity ψ and the ratio of shear and normal displacement u_0/v_0 for different values of E_1/E_2 are shown in Fig. 6 in the case of $a=0.75(\text{dm})$, $b=0.75(\text{dm})$, $h_1=h_2=0.1(\text{dm})$, $v_1=v_2=0.3$. The mode mixity ψ increases from zero when E_1/E_2 for different values of 1.0 in case of $u_0=0$.

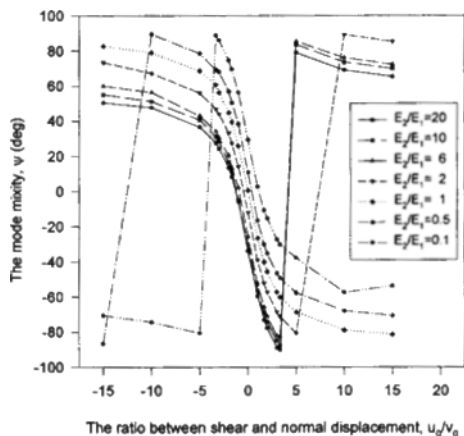


Fig. 6 Relationship between Ψ and u_0/v_0 for different ratios of E_1/E_2 and fixed parameters $a = b = 75$ (mm), $h_1 = h_2 = 10$ (mm), $\nu_1 = \nu_2 = 0.3$

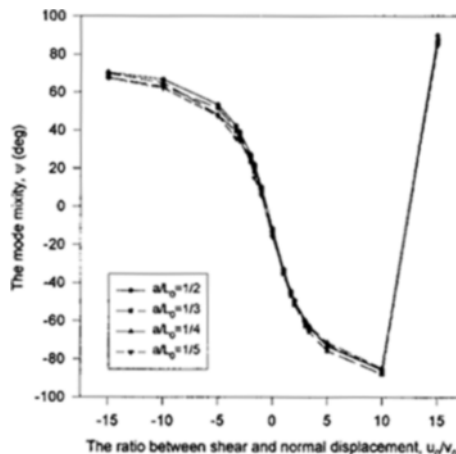


Fig. 8 Relationship between Ψ and u_0/v_0 for different ratios of a/L_0 , $L_0 = a + b = 150$ (mm), and fixed parameters $h_1 = h_2 = 10$ (mm), and $E_1 = 1.72$ GPa, $E_2 = 68.95$ GPa, $\nu_1 = 0.4$, $\nu_2 = 0.2$

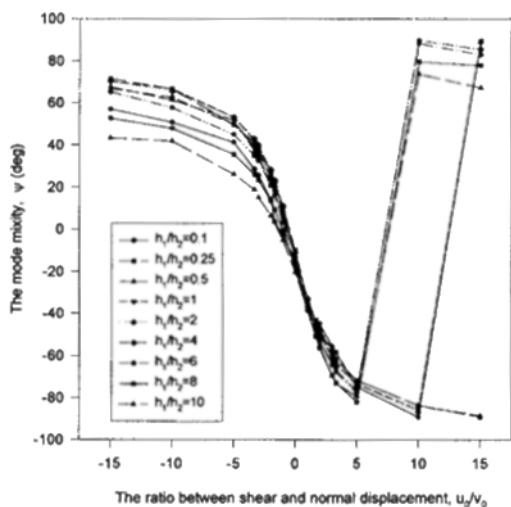


Fig. 7 Relationship between Ψ and u_0/v_0 for different ratio of h_1/h_2 and fixed parameters $a = b = 75$ (mm), $h_2 = 10$ (mm); and $E_1 = 1.72$ GPa, $E_2 = 68.95$ GPa, $\nu_1 = 0.4$, $\nu_2 = 0.2$

In Fig. 7, the relationship between Ψ and u_0/v_0 for different values of h_1/h_2 is shown in case of $a = b = 0.75$ (dm), and $E_1 = 1.72$ GPa, $E_2 = 68.95$ GPa, $\nu_1 = 0.4$, and $\nu_2 = 0.2$. When $u_0 = 0$, Ψ attains its maximum value when $h_1/h_2 = 1$, and decreases as h_1/h_2 which neither increases nor decreases.

Figure 8 shows the same curves for different crack lengths a/L_0 when $a + b = L_0 = 1.5$ (dm), $h_1 = h_2 = 0.1$ (dm), and $E_1 = 1.72$ GPa, $E_2 = 68.95$

GPa, $\nu_1 = 0.4$, $\nu_2 = 0.2$, and the values of Ψ are nearly constant under a specified loading condition.

The detailed meaning of these factors and theoretical predictions will be discussed later.

6. Conclusions

The crack opening displacements and energy release rate of the interface crack in bimaterial are calculated using analytical-variational method of solution and compared with experimental results. From this study the following conclusions can be made :

(1) All the basic governing equations in the theory of elasticity, boundary conditions on crack surfaces and conditions of continuity along interface are exactly satisfied by the expansions of displacement and stress fields.

(2) There is an oscillatory singularity of the stress field in the vicinity of the crack-tip and a penetration of displacements along both surfaces of crack, but in light of all the interface crack problems discussed in this paper, the size of the contact zone is so small that its effects can be ignored.

(3) The generalized stress intensity factors are

determined using the generalized variational principle. Due to the exact a priori satisfaction of all the basic governing equations, there are only line integrals in the variational equations, making the computations very simple and efficient, with good convergence of the GSIFs.

(4) The values of the crack opening displacement obtained in this theoretical approach are quite similar to those obtained in experiments.

Acknowledgment

The financial support of KOSEF for the Korea-China Post Doctoral Fellowship to Dr. Meng and the Yeungnam University Research Grant in 1996 is gratefully acknowledged. We would like to thank Dr. B. S. Choi and Prof. Y. S. Chai for helpful discussions.

References

- Choi, B. S and Chai, Y. S., 1995, "Experimental Analysis of Cracked along Bimaterial Interfaces," *Proceedings of ICCM-10*, Whistler, B. C., Canada, Vol. 1, pp. 285~292.
- Choi, H. J., 1994, "Stress Singularities in Dissimilar Orthotropic Composites Containing an Interlaminar Crack," *KSME Journal*, Vol. 8, No. 1, pp. 52~62.
- England, A. H., 1965, "A Crack Between Dissimilar Media," *J. Appl. Mech.*, Vol. 32, pp. 400~402.
- Erdogan, F., 1965, "Stress Distribution in Bonded Dissimilar Materials with Cracks," *J. Appl. Mech.*, Vol. 32, pp. 403~410.
- Malyshev, B. M. and Salganik, R. L., 1965, "The Strength of Adhesive Joints Using the Theory of Crack," *Inter. J. Frac. Mech.*, Vol. 1, pp. 114~128.
- Meng Qingchun and Zhang Xing, 1992, "Analytical-Generalized Variational Method of Solution for Delamination of Bi-metal Glued Joints," *Eng. Frac. Mech.*, Vol. 42, No. 1, pp. 73~78.
- Muskhelishvili, N. I., 1953, *Some Basic Problems of Mathematical Theory of Elasticity*, Noordhoff, Groningen.
- Qian Wei-chang, 1980, *Variational Methods and Finite Element Techniques*, Scientific Publishers of China.
- Rice J. R. and Sih G. C., 1965, "Plane Problem of Cracks in Dissimilar Media," *J. Appl. Mech.*, Vol. 32, pp. 418~423.
- Rice J. R., 1988, "Elastic Fracture Mechanics Concepts for Interfacial Cracks," *J. Appl. Mech.*, Vol. 55, pp. 98~103.
- Williams, M. L., 1959, "The Stress Around a Fault or Crack in Dissimilar Media," *Bull. Seismol. Soc. America*, Vol. 49, pp. 199~204.